Understanding the Reactivity of the Tetrahedrally Coordinated High-Valence d^0 Transition Metal Oxides toward the C−H Bond Activation of Alkanes: A Cluster Model Study

Gang Fu, Zhe-Ning Chen, Xin Xu,* and Hui-Lin Wan*

State Key Laboratory for Physical Chemistry of Solid Surfaces and Center for Theoretical Chemistry, Department of Chemistry & Institute of Physical Chemistry, Xiamen University, Xiamen, 361005, China

Received: October 2, 2007; In Final Form: October 29, 2007

We have carried out a theoretical study on the structure−function relationship for the selective oxidation of lower alkanes (C_1−C_4). The H abstraction mechanism has been examined over the model catalysts of high-valence d^0 transition metal oxides in the tetrahedral coordination. The intrinsic connections among the H abstraction barrier, the strengths of the O−H and the M−O bonds, the ability of electron transfer, as well as the energy gap of frontier orbitals of the oxides have been rationalized in terms of thermodynamics cycles and the frontier orbital analysis. In particular, we emphasize the role that the O−H bond strength plays in determining the reactivity of a metal oxide.

1. Introduction

Lower alkanes (C_1−C_4) are the main components in natural gas, coal bed gas, oil field associated gas, etc. Developing efficient strategies for the selective oxidation of lower alkanes to value-added chemicals or liquid fuels would provide a promising alternative for easing up the oil-demanding situation. Besides the well-known industrial process, i.e., the oxidation of *n*-butane to maleic anhydride, there are some other important examples under active investigation. These include the oxidation of methane to methanol or formaldehyde, oxidative dehydrogenation (ODH) of propane to propylene, (am)oxidation of propane to acrolein or acrylonitrile, etc. The common feature of these reactions is that all of them use the high-valence transition metal oxides, such as vanadium, chromium, molybdenum, and tungsten oxides, as catalysts.[1−3]

In most cases, the selective oxidation of hydrocarbons by oxides occurs through the so-called Mars−van Krevelen mechanism,[4−5] in which the organic molecule reacts with the lattice oxygen, and then the oxygen vacancy is replenished by gaseous oxygen. The roles that a good catalyst play involve (i) the effective activation of the first C−H bond, (ii) the directional transformation of the resulting intermediates into the partial oxidation product, and (iii) a fast reoxidation of the reduced surface. As a result, the redox properties of oxides influence their ability to complete such a catalytic cycle. Thus, the desire for developing a good catalyst with both high reactivity and selectivity calls for a molecular-level understanding of the redox properties of the oxides.

In the previous work,[6−9] we have carried out computational studies on lower alkane oxidations and concluded that the activation of a C−H bond usually proceeds via the H abstraction mechanism on a transition metal oxide

$$M^{n+}{=}O + H{-}R \rightarrow M^{(n-1)+}{-}O{-}H + R^{\bullet} \qquad (1)$$

Equation 1 shows that, when the C−H bond breaks, an O−H bond forms. Accordingly, the reaction enthalpy is equal to the difference of the C−H/O−H bond energies (BEs)

$$\Delta H_r = \mathrm{BE(C{-}H)} - \mathrm{BE(O{-}H)} \qquad (2)$$

Here, BE(C−H) and BE(O−H) are defined according to reactions 3 and 4, respectively

$$R{-}H \rightarrow R^{\bullet} + H^{\bullet} \qquad (3)$$

$$M^{(n-1)+}{-}O{-}H \rightarrow M^{n+}{=}O + H^{\bullet} \qquad (4)$$

In the radical chemistry, H abstraction is believed to be an enthalpy-driven process.[10−11] A fundamental question emerges as how to quantitatively characterize the reactivity of a specific oxygen site on surfaces. From the thermodynamic point of view, the strength of the resulting O−H bond is a suitable parameter. Theoretically, it is well established that hydrogen affinity could be used to probe the reactivity of different oxygen sites.[11−18] The recent cluster model,[17] as well as the periodic slab model calculations,[18] showed that the H atom is preferentially adsorbed on the terminal oxygen (=O). Moreover, by means of kinetic experiments, Mayer and co-workers concluded[19] that it is the hydrogen affinity that determined the ability of an oxide species to abstract an H atom. Since the formation of the O−H bond is accompanied by the reduction of the metal center formally by one unit, the O−H bond strength can thus be calculated from the thermodynamics cycle involving redox potential ($E°$) of $M^{n+}O/M^{(n-1)+}O$ and the pK_a of $M^{(n-1)+}O{-}H$.[20−22] However, such parameters are hard to be measured experimentally except for a few homogeneous oxo compounds. For easy use, people preferred to correlate the catalytic activity with some readily detected properties of metal oxides, such as the M−O bond energy[5,23−24] and the adsorption edge energy.[25]

Many authors have suggested[5,23−24] that the catalytic performance of oxides sensitively depends on the M−O bond energies, which can be deduced from the heats of formation of oxides, heats of adsorption/desorption, or parameters of isotopic exchange of oxygens. Actually, it has been found[23] that, with the decrease of the surface oxygen bond energy, the rate of total oxidation increases. However, Germain and Laugier pointed out[26] that such a correlation is not valid in the selective oxidation, indicating that the initial activation of the C−H bond is not directly related to the M−O bond strength in this case.

* To whom correspondence should be addressed. E-mail: xinxu@xmu.edu.cn (X.X.); hlwan@xmu.edu.cn (H.-L.W.).

10.1021/jp709651n CCC: $40.75
Published on Web 01/08/2008

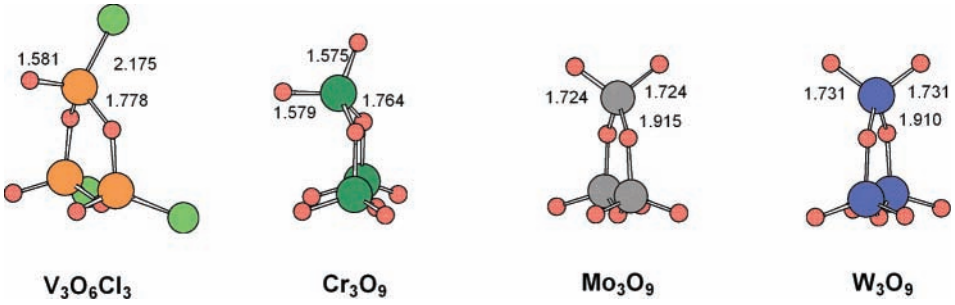

Figure 1. $V_3O_6Cl_3$ and M_3O_9 (M = Cr, Mo, W) cluster models, representing the high-valence d^0 transition metal oxides in the tetrahedral coordination. Yellow circle, V; green circle, Cr; gray circle, Mo; blue circle, W; red circle, O; red circle, O; light-green circle, Cl.

TABLE 1: Predicted Electronic Properties of M_3O_9 (M = Cr, Mo, W) and $V_3O_6Cl_3$ (873 K, Energy in kcal/mol and Bond Length in Angstrom)

	BE(O−H)[a]/R(O−H)		proton affinity[b]				
oxidants	=O	−O−	=O	−O−	electron affinity[c]	ΔE_{ST}[d]	BE(M=O)[e]
$V_3O_6Cl_3$	66.2/0.971	64.0/0.979	176.7	171.6	105.5	47.4	117.7
Cr_3O_9	84.9/0.977	75.7/0.979	169.6	167.0	112.8	32.5	82.3
Mo_3O_9	56.3/0.971	41.8/0.979	181.0	167.7	83.2	60.3	131.4
W_3O_9	43.3/0.963	26.7/0.980	179.2	153.9	75.4	74.5	158.9

[a] BE(O−H) = ΔH(M=O) + ΔH(H) − ΔH(M−O−H). [b] PA = ΔH(M=O) + $\Delta H(H^+)$ − $\Delta H(M-O-H^+)$. [c] EA = ΔH(M=O) − $\Delta H(M=O^-)$. [d] ΔE_{ST} = $\Delta H(M^{\bullet}-{}^{\bullet}O(\text{triplet}))$ − ΔH(M=O). [e] BE(M=O) = ΔH(M(triplet)) + $\Delta H(O(^3P))$ − ΔH(M=O).

TABLE 2: Calculated Barriers for H Abstraction from Lower Alkanes (873 K, kcal/mol)

		$V_3O_6Cl_3$		Cr_3O_9		Mo_3O_9		W_3O_9	
R−H	BE(C−H)	=O	−O−	=O	−O−	=O	−O−	=O	−O−
CH_3-H[8]	108.0	35.5	42.7	20.1	33.1	45.0	63.6	56.8	79.3
CH_3CH_2-H	103.2	29.8	36.6	14.3	25.7	36.5	55.7	50.0	70.0
$(CH_3)_2CH-H$	99.1	25.0	31.6	10.3	20.5	33.1	50.7	45.2	65.6
$(CH_3)_3C-H$	95.9	21.9	27.6	7.9	16.8	30.0	47.1	41.7	61.2

It is generally accepted that an effective activation of a C−H bond requires matching the orbital energies as well as the symmetry of the frontier orbitals between hydrocarbons and the oxide catalysts.[27] Bell et al. demonstrated[25] that the turnover rates of propane ODH are in parallel to the decrease of the energy of UV−vis absorption edge for all samples varying from NbO_x to WO_x, MoO_x, and VO_x. This implied that the reactivity of metal oxides is related to the gap between their valence and conductive bands, which, in turn, can be connected to their ability to transfer electrons from the lattice oxygens to the metal centers.

In this contribution, we report a theoretical study of the physicochemical properties of a series of metal oxides, including VO_x, CrO_x, MoO_x, and WO_x. We emphasize the role that the O−H bond strength plays in determining the reactivity of a metal oxide. The intrinsic connections among the strengths of the O−H bond and the M−O bond, the electron affinity, as well as the energy gap of the frontier orbitals are rationalized in terms of thermodynamics cycle and frontier orbital analysis.

2. Computational Methods

Here, we choose isostructural M_3O_9 (M = Cr, Mo, and W) and $V_3O_6Cl_3$ clusters as model catalysts (see Figure 1). Such models of choice not only fulfill the requirements of stoichiometry principle, neutrality principle, and coordination principle[28] but also are consistent with the experimental observations that metal oxide clusters themselves can serve as active centers in heterogeneous, homogeneous, and enzymatic catalysis.[29−31] In addition, similar cluster models have been successfully applied to the modeling of a variety of transition metal oxides catalyzed systems, including oxidations of methane, propane, and propylene, etc.[6−9,32−34]

The quantum calculations were performed by using hybrid density functional theory at the level of B3LYP.[35,36] Full geometry optimizations and analytical frequency calculations were performed with basis sets of double-ζ quality (6-31G)[37] for the main group elements. The final energies were calculated with polarization functions being included (6-31G**).[38] Hay's effective core potentials (Lanl2dz[39] denoted in Gaussian 03[40]) were used for transition metals, which included the relativistic effects for heavy metals. Energies reported here are enthalpies at 873 K and 1 atm, which generally correspond to the experimental conditions.

3. Results and Discussion

3.1. Correlating the Physicochemical Properties of Oxides with the O−H Bond Strength. It is widely accepted that the strength of the O−H bond is a key parameter[11,12,19] that controls the activation of the C−H bond over the metal oxide catalysts: The stronger the O−H bond forms, the more rapid the reaction between the hydrocarbon molecule and the oxide surface. Our calculation results are summarized in Table 1, which shows that the lengths of the as-formed O−H bonds are between 0.96 and 0.98 Å for different oxygen sites of different metals, whereas the strengths of the O−H bonds vary from 26.7 to 84.9 kcal/mol. The general trends can be summarized as follows: (1) The strength of the O−H bond decreases down the column from Cr to Mo, and to W, while that of V is in between Cr and Mo. (2) H adsorption on a terminal oxygen is favored over that on a bridge oxygen for a given metal. (3) The difference of the O−H bond strength between the terminal oxygen and the bridge oxygen is pronounced, while that for the V oxide is mild. There are many factors that contribute to the strength of an O−H bond. Since an H atom can be viewed as a combination of an electron

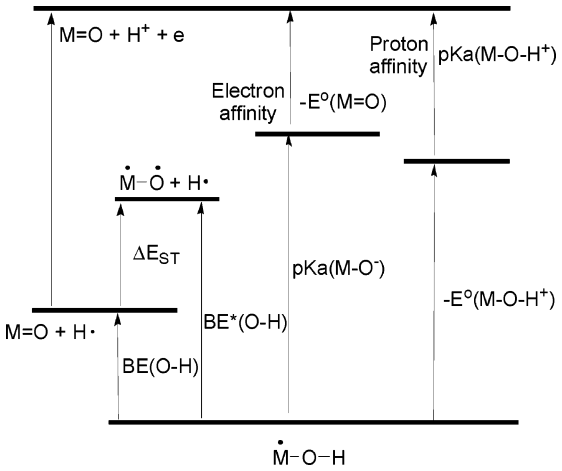

Figure 2. Thermodynamics cycle involved in forming an O−H bond between H atom and M═O.

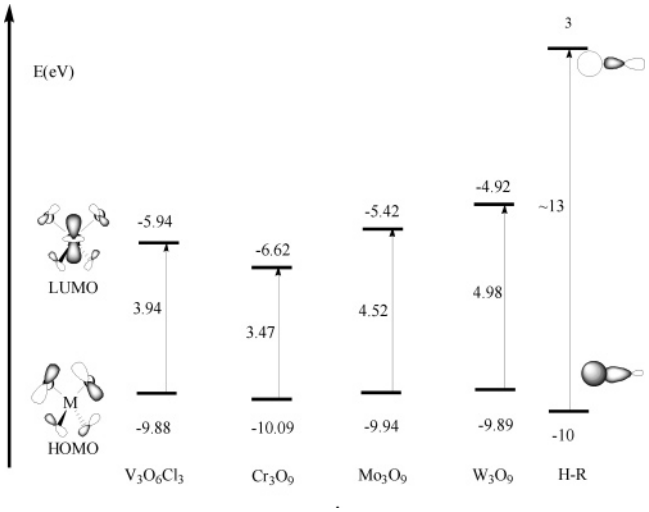

Figure 3. Frontier orbitals of the high-valence d^0 transition metal oxides in the tetrahedral coordination. A localized picture of a C−H bond is also shown. The calculated HOMO and LUMO energies are −10.61 and 3.19 eV for CH_4, −9.26 and 2.83 eV for C_2H_6, −8.82 and 2.59 eV for C_3H_8, and −8.63 and 2.32 eV for *i*-C_4H_{10}, respectively.

and a proton,[22,41,42] the strength of an O−H bond shall be correlated not only with the electron affinity but also with the proton affinity. As the formation of an O−H bond couples with the breakage of an M═O bond, a weaker M═O π bond shall lead to a higher H affinity. Thermodynamics cycles involving such processes are illustrated in Figure 2.

A process of PCET (proton-coupled electron transfer[22,41,42]) differs from that of the H transfer in that the destination of the proton and the electron can be different. Hence, in PCET, the metal center can be the electron acceptor, whereas the oxygen can act as the proton acceptor. Table 1 summarizes the electron affinity and proton affinity of various oxides. As the additional electron will occupy the lowest unoccupied molecular orbital (LUMO), which normally corresponds to the $\pi^*_{M=O}$ orbital for a tetrahedrally coordinated d^0 transition metal oxide, the central metal is formally reduced by one unit. Therefore, electron affinity is naturally associated with the reducibility of the metal center. Our calculations show that the reducibility decreases from Cr to V, to Mo, and to W, in parallel with the sequence of decreasing strength of the O−H bonds (see Table 1).

Protons can be stabilized on both the terminal oxygen and the bridge oxygen sites, as shown by the large proton affinities

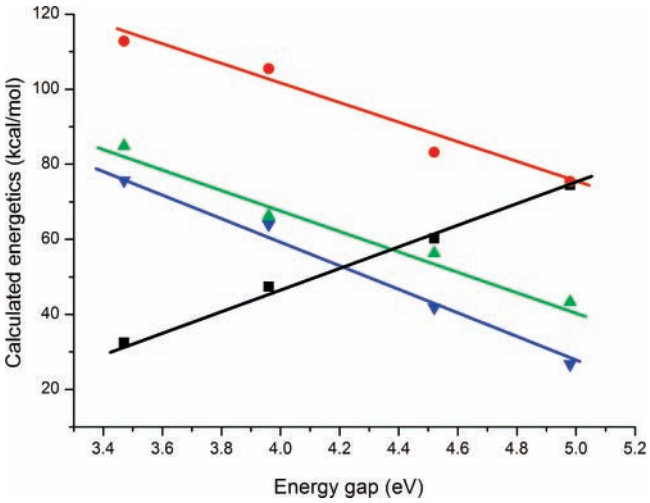

Figure 4. Plots of ΔE_{ST}, EA, and BE(O−H) vs the energy gap between HOMO and LUMO of the high-valence d^0 transition metal oxides in the tetrahedral coordination. Black squares, ΔE_{ST}; blue triangles, O−H bond (−O−); green triangles, O−H bond (═O); red circles, EA.

(PAs) in Table 1. From these data, the following trends can be noticed: (1) Generally, PA to a terminal oxygen is larger than that to a bridge oxygen for a given oxide. (2) For V and Cr, PAs of both sites are comparable, whereas for Mo and W, PAs differ significantly between these two kinds of oxygen. (3) For the terminal oxygen site, PAs are roughly the same for V, Mo, and W oxides, which are around 10 kcal/mol higher than those for the Cr oxide. (4) For the bridge oxygen site, PAs are roughly the same for V, Cr, and Mo oxides with the exception of the W oxide, whose PA is around 13 kcal/mol smaller than the others. Most significantly, we see that, for different oxides, PAs have no correlation with the trends of the strength of the O−H bonds, whereas for a given oxide, PA difference can be used to qualitatively differentiate the O−H binding energy difference between the terminal oxygen and the bridge oxygen site (see Table 1).

Table 1 also lists the predicted singlet−triplet excitation energies, ΔE_{ST}(M═O), as well as the M═O bond energy, BE-(M═O). For a high-valence d^0 transition metal oxide, the singlet−triplet excitation, involving an electron transfer from the highest occupied molecular orbital (HOMO) to LUMO, will give rise to an oxyradical ($M^{\bullet}-O^{\bullet}$). ΔE_{ST} is usually used to estimate the strength of the M═O π bond.[43] We find that for the first-row transition metal oxides, such as V and Cr, the π bond strengths are relatively weak. The π bond becomes stronger, as the metal goes down the column, Cr < Mo < W. Interestingly, Grasselli suggested[44] that the resonance structure of the vanadyl moiety (V^{5+}═O ↔ $^{4+}V^{\bullet}-O^{\bullet}$) is important in the activation of alkanes in the Mo−V−Nb−Te−O_x system, indicating that the reactivity of the oxides is strongly influenced by the M═O π bond strength. As shown in Figure 2, we may define BE*(O−H) as the bond energy between H and the triplet $M^{\bullet}-O^{\bullet}$. Hence, BE*(O−H) is equal to the sum of ΔE_{ST}(M═O) and BE(O−H). From Table 1, we can calculate that, for various oxides under the present study, the values of BE*(O−H) are nearly a constant (113.6−117.8 kcal/mol). Thus, ΔE_{ST} can be written as

$$\Delta E_{ST}(\text{M=O}) = \text{constant} - \text{BE(O-H)} \qquad (5)$$

Equation 5 suggests that the O−H bond energy on a terminal oxygen site is inversely proportional to the singlet−triplet excitation energies ΔE_{ST}(M═O).

Detaching an oxygen atom (^{3}P) from a terminal oxygen site involves breaking not only a π bond but also a σ bond, eventually leading to the formation of an oxygen vacancy. The heat of such a process can be correlated to BE(M═O). Here, we find that the strength of BE(M═O) follows the same trend with ΔE_{ST}, deceasing from W to Mo, to V, and then to Cr (see Table 1). It should be emphasized that the catalytic performance of the oxide can be subtly tuned by the strength of the M═O bond.[45−47] When the M═O bond is too weak, such as a Cr═O, regeneration of the lattice oxygen can be a big issue in order to complete the Mars−van Krevelen mechanism. If the M═O bond is too strong, such as W═O, the penalty to open the M═O π bond is too high, such that abstracting an H atom from alkanes can be hard to accomplish. The requirement of a good catalyst is only fulfilled when the metal oxide can have an appropriate M═O bond, such as those in the V and Mo oxides. This finding is in accord with the experimental observation[3,5] that the M═O bond must be of intermediate strength to carry out the selective oxidation catalysis.

The concept of frontier orbital interaction is widely accepted and applied in predicting the feasibility of a chemical reaction. Figure 3 displays the frontier orbitals of various high-valence d^0 transition metal oxides in the tetrahedral coordination. These orbitals are compared with the bonding and antibonding orbitals of a C−H in alkanes. We can see that the HOMOs of oxides have a nonbonding character located only on the oxygen atoms, while the LUMOs have a dominant $\pi^*_{M=O}$ character. Our calculations show that the positions of the HOMOs for different oxides are roughly the same (−10.09 to −9.88 eV), but the energies of the LUMOs vary from −6.62 to −4.92 eV. Thus, promoting an electron from HOMO to LUMO (ΔE_{ST}) is mainly determined by the energy level of LUMO. Hence, ΔE_{ST}(M═O) correlates well with EA. The plots of BE(O−H), electron affinities, ΔE_{ST}, and BE(M═O) vs the HOMO/LUMO energy gap are depicted in Figure 4. We can see that ΔE_{ST} increases in parallel with the energy gap, while EA decreases monotonically as the energy gap increases, in consistency with the frontier orbital analysis. Importantly, Figure 4 clearly demonstrates that BE(O−H) on both the terminal oxygen and the bridge oxygen sites correlate well with the energy gap, albeit with different slope. While ΔE_{ST} has the limitation to only be applicable to the estimation of the M═O π bond, which, in turn, correlates only with BE(O−H) on the terminal oxygen sites, the frontier orbital energy gap and EA are global properties of oxides, which can be correlates to BE(O−H) on both the terminal oxygen and the bridge oxygen site.

3.2. Correlations between the Reactivity and the Redox Features. Table 2 summarizes the predicted H abstraction barriers of lower alkanes, varied from methane to *i*-butane, over the oxides of V, Cr, Mo, and W. The general trends for the H abstraction pathways can be summarized as the following: (1) For a given R−H, the reactivity decreases in the order of Cr, V, Mo, and W, as the calculated barriers increase in this series. This correlates well with the trend of the O−H bond strengths. (2) For a given oxide, H abstractions by [═O] are favored over those by [−O−], in consistency with the relative strength of BE(O−H) and PA of these two sites. (3) The reactivity of different alkanes follows the trend of $(CH_3)_3C-H > (CH_3)_2CH-H > CH_3CH_2-H > CH_3-H$, antiparallel to the strength of the broken C−H bond. From eqs 1 and 2, we see that the O−H bond strength provides a useful criterion to measure the reactivity of different oxides as well as different sites.

Figure 5 plots the correlation of the calculated H abstraction barriers vs the reaction enthalpy deduced from eq 2. We find a good linearity (correlation coefficient $R^2 = 0.974$) with a slope of 0.943, reinforcing the idea that M═O behaves like an oxygen radical, even though it is not a radical.[19] And we also find that some points scatter around the linear correlation with ±4 kcal/mol errors. Many factors will contribute to this deviation. (1) H abstraction by a bridge [−O−] will disturb the M−O σ bond, which is stronger than the corresponding M═O π bond. (2) The electrostatic interaction between the metal oxide and the alkane molecule make a considerable contribution in stabilizing the transition state (TS). (3) The polar effect in the TS results in the stability of the $[C^+\cdots H\cdots O^-]$ configuration, which reduces the barrier to a greater extent[48−50] with the H atoms of CH_4 being sequentially replaced by the CH_3 group, i.e., from CH_3-H to $(CH_3)_3C-H$.

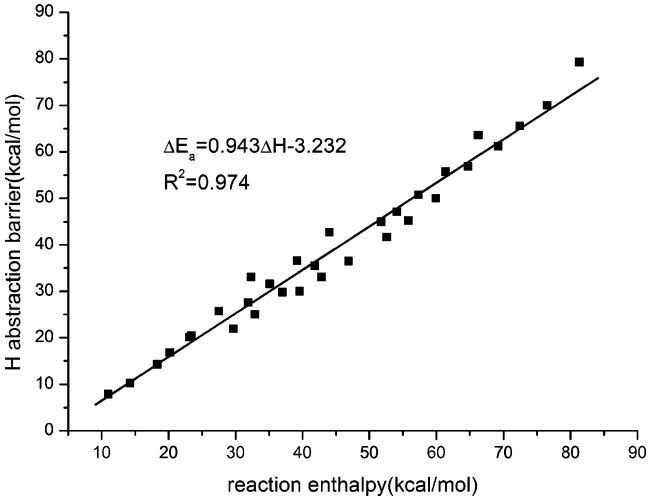

Figure 5. Plot of the calculated H abstraction barrier vs the corresponding reaction enthalpy.

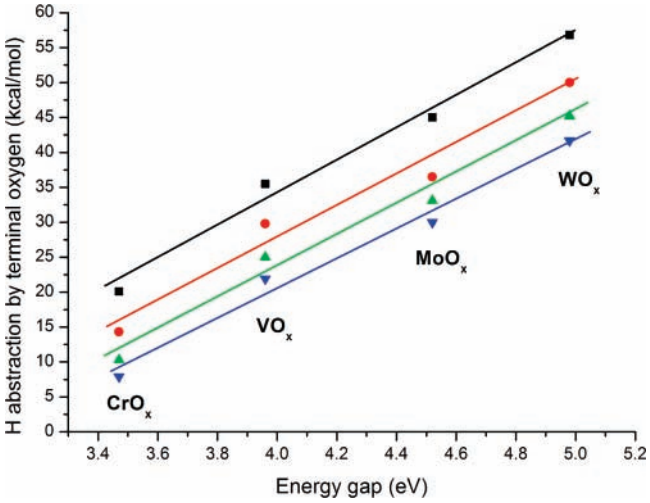

Figure 6. Plots of the H abstraction barrier for a given C−H bond vs the energy gap of oxides. Black squares, CH_3-H; red circles, CH_3-CH_2-H; green triangles, $(CH_3)_2CH-H$; blue triangles, $(CH_3)_3C-H$.

Alkane molecules possess a low EA, such that LUMO of a C−H bond is high lying (see Figure 3). It is thus; the HOMOs of alkanes match the LUMOs of the metal oxides to achieve the C−H bond oxidation. Accordingly, we find that the H abstraction barriers are closely related to the energy gaps of oxides, as shown in Figure 6. For a given R−H, the calculated barriers increase from Cr to V, to Mo, and to W, in good agreement with the increased tendency of the energy gap. This finding corroborates Bell's proposal[28] that rates of alkane

oxidation can be roughly correlated with the UV−vis absorption edge of the oxide catalysts.

4. Conclusion

It is well known that the catalytic performance of selective oxidation relies on the ability of oxides to provide the surface oxygen as a reactant. Here we present a theoretical study to elucidate the relationship between the reactivity and physicochemical properties of the active oxygen center. We disclose that transition metal oxides behaves like free radicals, which can abstract an H atom from alkanes to give a surface hydroxyl group (O−H). We conclude that the H abstraction barrier can correlate well with the reaction enthalpy as the difference of BE(C−H) and BE(O−H). Thus, for a given alkane, the strength of the O−H bond plays a central role in determining the reactivity of the metal oxide. We find that the O−H bond strength, EA, and ΔE_{ST} are critically dependent on the HOMO/LUMO energy gap of the oxide. When the energy gap increases, ΔE_{ST} increases monotonically, and both the O−H bond strength and EA decrease monotonically.

Acknowledgment. This work was supported by National Natural Science Foundation of China (20525311, 20533030, 20503022, 20433030), the Ministry of Science and Technology (2005CB221408, 2004CB719902, 2007CB815206). and the Key Scientific Project of Fujian Province of China (2005 HZ01-3).

References and Notes

(1) *Selective Oxidation by Heterogeneous Catalysis*; Centi, G., Cavani, F., Trifirò, F., Eds.; Kluwer Academic/Plenum Publishers: New York, 2001.
(2) *Handbook of Heterogeneous Catalysis*; Ertl, G., Knoezinger, H., Weitkamp, J., Eds.; J. Wiley-VCH: Weinheim, Germany, 1997; Vol. V.
(3) Grzybowska-Świerkosz, B. *Top. Catal.* **2000**, *11/12*, 23.
(4) Mars, P.; van Krevelen, D. W. *Chem. Eng. Sci. Suppl.* **1954**, *3*, 3.
(5) Grasselli, R. K. *Top. Catal.* **2002**, *21*, 79.
(6) Fu, G.; Xu, X.; Lu, X.; Wan, H. *J. Am. Chem. Soc.* **2005**, *127*, 3989.
(7) Fu, G.; Xu, X.; Lu, X.; Wan, H. *J. Phys. Chem. B* **2005**, *109*, 6416.
(8) Fu, G.; Xu, X.; Wan, H. *Catal. Today* **2006**, *117*, 133.
(9) Fu, G.; Yi, X.; Huang, C.; Xu, X.; Weng, W.; Xia, W.; Wan, H. *Surf. Rev. Lett.* **2007**, *14*, 645.
(10) Fokin, A. A.; Schreiner, P. R. *Chem. Rev.* **2002**, *102*, 1551.
(11) Siegbahn, P. E. M.; A Blomberg, M. R.; Crabtree, R. H. *Theor. Chem. Acc.* **1997**, *97*, 289.
(12) Witko, M. *Catal. Today* **1996**, *32*, 89.
(13) Hermann, K.; Michalak, A.; Witko, M. *Catal. Today* **1996**, *32*, 321.
(14) Witko, M.; Hermann, K.; Tokarz-Sobieraj, R. *Catal. Today* **1999**, *50*, 553.
(15) Hermann, K.; Chakrabarti, A.; Druzinic, R.; Witko, M. *Phys. Status Solidi A* **1999**, *173*, 195.
(16) Hermann, K.; Witko, M.; Druzinic, R. *Faraday Discuss.* **1999**, *53*, 53.
(17) Hermann, K.; Witko, M.; Druzinic, R.; Tokarz, R. *Top. Catal.* **2001**, *11/12*, 67.
(18) Yin, X.; Han, H.; Endou, A.; Kubo, M.; Teraishi, K.; Chatterjee, A.; Miyamoto, A. *J. Phys. Chem. B* **1999**, *103*, 1263.
(19) Mayer, J. M. *Acc. Chem. Res.* **1998**, *31*, 441.
(20) Parker, V. D.; Handoo, K. L.; Roness, F.; Tilset, M. *J. Am. Chem. Soc.* **1991**, *113*, 7493.
(21) *Biomimetic Oxidations Catalyzed by Transition Metal Complexes*; Meunier, B., Eds.; Imperial College: London, 2000; pp 1−43.
(22) Mayer, J. M. *Annu. Rev. Phys. Chem.* **2004**, *55*, 363.
(23) Moro-Oka, Y.; Ozaki, A. *J. Catal.* **1966**, *5*, 116.
(24) Grzybowska-Świerkosz, B. *Top. Catal.* **2002**, *21*, 35.
(25) Chen, K.; Xie, S.; Bell, A. T.; Iglesia, E. *J. Catal.* **2000**, *195*, 244.
(26) Germain, J. F.; Laugier, R. *Bull. Soc. Chim. Fr.* **1972**, 541.
(27) Haber, J.; Witko, M. *J. Catal.* **2003**, *216*, 416.
(28) Xu, X.; Nakatsuji, H.; Lu, X.; Ehara, M.; Cai, Y.; Wang, N. Q.; Zhang, Q. E. *Theor. Chem. Acc.* **1999**, *172*, 170.
(29) Fialko, E. F.; Kikhtenko, A. V.; Goncharov, V. B. *Organometallics* **1998**, *17*, 25.
(30) Hill, C. L.; Prosser-McCartha, C. M. *Coord. Chem. Rev.* **1995**, *143*, 407.
(31) Yang, W.; Wang, X.; Guo, Q.; Zhang, Q.; Wang, Y. *New J. Chem.* **2003**, *27*, 1301.
(32) Cheng, M.; Chenoweth, K.; Oxgaard, J.; van Duin, A.; Goddard, W. A. *J. Phys. Chem. C* **2007**, *111*, 5115.
(33) Jang, Y. H.; Goddard, W. A. *Top. Catal.* **2001**, *1*, 273.
(34) Jang, Y. H.; Goddard, W. A. *J. Phys. Chem. B* **2002**, *106*, 5997.
(35) Becke, A. D. *Phys. Rev. A* **1988**, *38*, 3098.
(36) Lee, C. T.; Yang, W. T.; Parr, R. G. *Phys. Rev. B* **1988**, *37*, 785.
(37) Hehre, W. J.; Ditchfield, R.; Pople, J. A. *J. Chem. Phys.* **1972**, *56*, 2257.
(38) Hariharan, P. C.; Pople, J. A. *Theor. Chim. Acta.* **1973**, *28*, 213.
(39) Hay, P. J.; Wadt, W. R. *J. Chem. Phys.* **1985**, *82*, 299.
(40) Frisch, M. J.; Trucks, G. W.; Schlegel, H. B.; Scuseria, G. E.; Robb, M. A.; Cheeseman, J. R.; Montgomery, J. A., Jr.; Vreven, T.; Kudin, K. N.; Burant, J. C.; Millam, J. M.; Iyengar, S. S.; Tomasi, J.; Barone, V.; Mennucci, B.; Cossi, M.; Scalmani, G.; Rega, N.; Petersson, G. A.; Nakatsuji, H.; Hada, M.; Ehara, M.; Toyota, K.; Fukuda, R.; Hasegawa, J.; Ishida, M.; Nakajima, T.; Honda, Y.; Kitao, O.; Nakai, H.; Klene, M.; Li, X.; Knox, J. E.; Hratchian, H. P.; Cross, J. B.; Bakken, V.; Adamo, C.; Jaramillo, J.; Gomperts, R.; Stratmann, R. E.; Yazyev, O.; Austin, A. J.; Cammi, R.; Pomelli, C.; Ochterski, J. W.; Ayala, P. Y.; Morokuma, K.; Voth, G. A.; Salvador, P.; Dannenberg, J. J.; Zakrzewski, V. G.; Dapprich, S.; Daniels, A. D.; Strain, M. C.; Farkas, O.; Malick, D. K.; Rabuck, A. D.; Raghavachari, K.; Foresman, J. B.; Ortiz, J. V.; Cui, Q.; Baboul, A. G.; Clifford, S.; Cioslowski, J.; Stefanov, B. B.; Liu, G.; Liashenko, A.; Piskorz, P.; Komaromi, I.; Martin, R. L.; Fox, D. J.; Keith, T.; Al-Laham, M. A.; Peng, C. Y.; Nanayakkara, A.; Challacombe, M.; Gill, P. M. W.; Johnson, B.; Chen, W.; Wong, M. W.; Gonzalez, C.; Pople, J. A. *Gaussian 03*, revision D.01; Gaussian, Inc.: Wallingford, CT, 2004.
(41) Cukier, R. I.; Nocera, D. G. *Annu. Rev. Phys. Chem.* **1998**, *49*, 337.
(42) Hammes-Schiffer, S. *Acc. Chem. Res.* **2001**, *34*, 273.
(43) Xu, X.; Faglioni, F.; Goddard, W. A. *J. Phys. Chem. A* **2002**, *106*, 7171.
(44) Grasselli, R. K.; Burrington, J. D.; Buttrey, D. J.; DeSanto, P., Jr.; Lugmair, C. G.; Volpe, A. F., Jr.; Weingand, T. *Top. Catal.* **2003**, *23*, 5.
(45) Holm, R. H. *Chem. Rev.* **1987**, *87*, 1401.
(46) Holm, R. H.; Donahue, J. P. *Polyhedron* **1993**, *12*, 571.
(47) Enemark, J. H.; Cooney, J. j. A.; Wang, J. J.; Holm, R. H. *Chem. Rev.* **2004**, *104*, 1175.
(48) Kochi, J. K. *Free radicals*; Wiley: New York, 1973.
(49) Tedder, J. M. *Angew. Chem., Int. Ed. Engl.* **1982**, *21*, 401.
(50) Roberts, B. P. *Chem. Soc. Rev.* **1999**, *28*, 25.